

First-principles study of α -Pu₂O₃

Hongliang Shi^{1,2} and Ping Zhang^{1,3,*}

¹*Institute of Applied Physics and Computational Mathematics,
P.O. Box 8009, Beijing 100088, People's Republic of China*

²*SKLSM, Institute of Semiconductors, Chinese Academy of Sciences,
P. O. Box 912, Beijing 100083, People's Republic of China*

³*Center for Applied Physics and Technology, Peking University, Beijing 100871, People's Republic of China*

We systematically investigate the electronic structure, magnetic order, and valence states of α -Pu₂O₃ (*C*-type) by using first-principles calculations. α -Pu₂O₃ can be constructed from PuO₂ by removing 25% oxygen atoms. Our results show that the Pu 5*f* orbitals are further localized after removing ordered oxygen atoms. This phenomenon is demonstrated by the combined fact that (i) the volume per unit cell expands 7% and (ii) the corresponding magnetic moments and valence states for Pu ions increase and decrease, respectively. According to the density of states and charge density distribution analysis, PuO₂ is found to be more covalent than α -Pu₂O₃, which is also because of the more localization of 5*f* orbitals in the latter. The calculated lattice constants, bulk modulus, and electronic structures for PuO₂ and α -Pu₂O₃ are consistent well with experimental observations.

PACS numbers: 71.27.+a, 71.15.Mb, 71.20.-b

I. INTRODUCTION

Plutonium-based materials have been extensively investigated because of not only their great technological importance in the nuclear industry application but also their interesting rich physical properties from the basic theoretical viewpoint. Metallic Pu locates in the boundary of localized and delocalized 5*f* electrons among the actinide metals and it has six different phase under different temperatures and pressures because of the complex character of the 5*f* electrons [1, 2]. As for plutonium oxides, which are the only products when metallic plutonium is exposed in air, can store the surplus metallic plutonium [3]. The corrosion oxidation of metallic plutonium in air is very hot topic since it is a key problem for the protection and storage of plutonium-based nuclear weapons. Furthermore, the thermodynamics and redox properties of plutonium oxides are also complex and interesting. When Pu is exposed to dry air at room temperature, the plutonium dioxide PuO₂ layer is formed and a thin layer of plutonium oxide Pu₂O₃ is followed on plutonium surfaces [3]. After several months or years, most of the PuO₂ layer auto-reduces into Pu₂O₃ layer. Especially, at 150-200°C, all the PuO₂ layer auto-reduces into Pu₂O₃ layer in minutes [3]. Usually, the mentioned plutonium sesquioxide is β -Pu₂O₃ in the hexagonal structure (*P* $\bar{3}m1$). However, another abnormal body centered cubic form, plutonium sesquioxide PuO_{1.52}, was also detected [4]. The ideal stoichiometric cubic plutonium sesquioxide is α -Pu₂O₃ (*C*-type PuO_{1.5}), which are consisted of 32 Pu atoms and 48 O atoms per unit cell. α -Pu₂O₃ has not been prepared as a single-phase compound, since it is stable only below 300°C [5]. A mixture

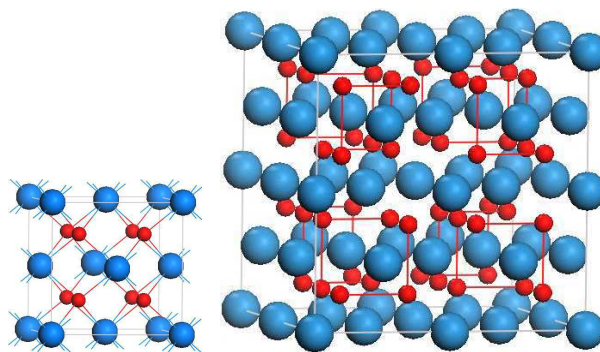


FIG. 1: (left) unit cell of PuO₂ with CaF₂-type structure. (right) unit cell of α -Pu₂O₃ (body-centered cubic). The blue and red spheres denote Pu and O atoms, respectively.

of cubic PuO_{1.52} and PuO_{1.98} can be obtained by partial reduction of PuO₂ at high temperature and cooling to room temperature [5].

Naturally, the reduction of PuO₂ into α -Pu₂O₃ is easy to happen because of the similarity of their cubic structures. PuO₂ crystallizes in the CaF₂ structure (see Fig. 1) with the plutonium and oxygen atoms forming face-centered and simple cubic sublattices, respectively, and the cubic α -Pu₂O₃ can be obtained from PuO₂ 2×2×2 supercell after removing ordered 25% oxygen atoms [3]. Actually, the structure of α -Pu₂O₃ is body-centered cubic with space group *Ia* $\bar{3}$ (No.206). Oxygen atoms occupy the 48*e* sites, and plutonium atoms occupy the 24*d* and 8*a* sites [5] (see Fig. 1). Furthermore, if the 16*c* sites are also occupied by oxygen atoms, the resulting cell is the same as PuO₂ 2×2×2 supercell. Therefore, as mentioned above, the cubic α -Pu₂O₃ can be obtained by removing oxygen atoms located in the 16*c* (0.25,0.25,0.25) sites.

In this work, we pay special attention to how the electronic structure, magnetic order, and Pu valence states change during the PuO₂-Pu₂O₃(α) reduction process. In

*Author to whom correspondence should be addressed. Electronic address: zhang-ping@iapcm.ac.cn

PuO_2 , Pu is in the ideal stable +4 oxidation state while in $\alpha\text{-Pu}_2\text{O}_3$ the ideal oxidation state is +3. This change of valence states may illustrate that the $5f$ electrons are more localized in $\alpha\text{-Pu}_2\text{O}_3$. Similar to $\text{CeO}_2\text{-Ce}_2\text{O}_3$ reduction transition [6], after creating one oxygen vacancy, two electrons left behind are condensed into localized f -level traps on two plutonium atoms, therefore, the valence for Pu changes from +4 to +3. Furthermore, due to the localization our results show that the volume expands 7% during $\text{PuO}_2\text{-Pu}_2\text{O}_3$ isostructure reduction process.

In order to describe more accurately the strong on-site Coulomb repulsion interaction among the plutonium $5f$ electrons, we use the generalized gradient approximation (GGA)+ U scheme. Our previous studies showed that the GGA+ U approach can accurately describe the electronic structures and thermodynamic properties of PuO_2 and $\beta\text{-Pu}_2\text{O}_3$ [8], which has motivated more theoretical calculations in these two years [10, 11, 12]. In the following, our calculated results demonstrate that the GGA+ U correction can also successfully predict the ground state properties of cubic $\alpha\text{-Pu}_2\text{O}_3$ and reliably describe the $\text{PuO}_2\text{-Pu}_2\text{O}_3(\alpha)$ reduction process. Our study shows that the system's volume expands during the reduction process. Also, two well-resolved peaks in the density of states (DOS) are observed and identified to originate from the Pu $5f$ and O $2p$ states in PuO_2 , which are consistent well with the recent photoemission measurements [9]. In addition, our calculated bulk modulus for PuO_2 is 180 GPa with Hubbard $U=3.0$ eV, which agrees excellently with the recent refined experimental values of 178 GPa [13]. However, in Ref. [14], this value is largely overestimated to be 379 GPa.

II. DETAILS OF CALCULATION

Our first-principles calculations are based on the density functional theory (DFT) and the Vienna ab initio simulation package (VASP) [15] using the GGA for the exchange correlation potential [16]. The electron and core interactions are included using the frozen-core projected augmented wave (PAW) approach which combines the accuracy of augmented-plane-wave methods with the efficiency of the pseudo-potential approach [17]. The Pu $5f$, $6s$, $6p$, $6d$, and $7s$ as well as the oxygen $2s$ and $2p$ electrons are explicitly treated as valence electrons. The electron wave function is expanded in plane waves up to a cutoff energy of 500 eV. For the Brillouin zone integration, the $2\times 2\times 2$ Monkhorst-Pack sampling is adopted. The strong on-site Coulomb repulsion among the localized Pu $5f$ electrons is described by using the formalism formulated by Dudarev *et al.* [7]. In this scheme, only the difference between the spherically averaged screened Coulomb energy U and the exchange energy J is important for the total LDA (GGA) energy functional. Thus, in the following we label them as one single effective parameter U for brevity. In our calculation, we use $J=0.75$ eV for the exchange energy, which is close to the values

used in other previous work [8, 11].

III. RESULTS AND DISCUSSIONS

A. Atomic and electronic structure of PuO_2

In order to investigate the electronic and structural properties of $\alpha\text{-Pu}_2\text{O}_3$ and how these properties change during the reduction process from PuO_2 to $\alpha\text{-Pu}_2\text{O}_3$, it is essential to first calculate the corresponding properties of PuO_2 . Table I shows our calculated lattice constant a_0 and bulk modulus B_0 and its pressure derivative B'_0 within GGA+ U scheme with different Hubbard U parameters. We performed the ferromagnetic (FM) and anti-ferromagnetic (AFM) coupling calculations to decide which is the ground state according to the total energies for each choice of the Hubbard U value. PuO_2 is known to be an insulator [18] and some scattered experimental data proved its ground state to be an AFM phase [19]. For bare GGA, i.e., $U=0$ eV, our calculated result predicts PuO_2 to be a FM metal, similar to the conclusion of previous studies. This is contrary to experimental observation. By increasing the amplitude of U , as shown in Fig. 2, the total energy difference between the two phases decreases; the AFM phase begins to be energetically preferred at $U\sim 1.5$ eV. We find that the convergence to the correct AFM phase is very rapid. Taking $U=3.0$ eV, for example, the total energy (per formula unit) for the AFM phase is lower than for the FM phase by a large value of 0.4 eV. Note that in our calculation of PuO_2 in this section, we have chosen two kinds of magnetic configurations. One is that the Pu magnetic moments μ are confined along the z axis in a simple $+-+-$ alternation of spins, while the other is the interlayer alternation of spins. Our results show that the total energies for the two configurations are degenerate. In the ideal ionic limit, the formal charge for Pu ions in PuO_2 is +4, corresponding to the formal population of f^4 for f orbitals. Our direct calculated magnetic moments μ for each plutonium ion is 4.16 (in unit of Bohr magneton) mainly contributed by $4f$ orbitals of 4.09, which is very close to the population of f^4 .

The equilibrium lattice constant a_0 and bulk modulus B_0 and its pressure derivative B'_0 are obtained by fitting the Murnaghan equation of state [20]. At $U=3.0$ and 4.0 eV, the present lattice constants a_0 are 5.458 and 5.477 Å for the AFM phase, respectively, which are in good agreement with the experimental value of 5.396 Å [21]. As for the bulk modulus, our calculated results are 180 and 184 GPa with $U=3.0$ and 4.0 eV, respectively, which agree well with the recent refined experimental value of 179 GPa. However, in an early experiment [14], this value is largely overestimated to be 379 GPa. Notice that the results of lattice constant and bulk modulus are 5.46 Å and 220 GPa, respectively, which are obtained using hybrid-density-functional calculations [22]. The physical insulating behavior of PuO_2 with an experimentally

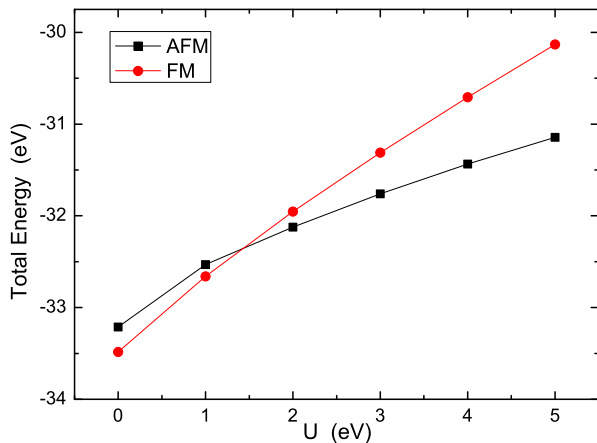


FIG. 2: The total energies for PuO_2 in FM and AFM phases with different Hubbard U parameters.

TABLE I: Calculated and experimental lattice constants a_0 (Å) and bulk modulus B (GPa) for Pu_2O_3 and PuO_2 by the GGA+ U scheme.

	U (eV)	order	a_0 (Å)	B_0 (GPa)	B'_0
PuO_2	4.0	FM	5.454	184	3.72
	4.0	AFM	5.477	184	3.72
	3.0	FM	5.438	183	4.72
	3.0	AFM	5.458	180	4.68
	0	FM	5.386	193	3.95
	0	AFM	5.398	187	3.67
	Expt.		5.396		
Pu_2O_3	0	FM	10.91	133	5.52
	0	AFM	10.92	123	4.25
	3.0	FM	11.14	119	4.05
	3.0	AFM	11.17	122	3.82
	4.0	FM	11.18	120	3.91
	4.0	AFM	11.20	128	3.31
	Expt.		11.05		

comparable Mott gap of ~ 1.5 eV has as well been obtained with Hubbard U in a range of 3-4 eV. Therefore, our GGA+ U results can provide a satisfactory description of the atomic, mechanical, electronic, and magnetic (FM or AFM) structures of PuO_2 . This encourages us to investigate in the following the ground-state properties of $\alpha\text{-Pu}_2\text{O}_3$ by the same method, which turns to be remarkably effective as well. The present calculation of PuO_2 is also necessary for theoretical access to the $\text{PuO}_2 \leftrightarrow \text{Pu}_2\text{O}_3(\alpha)$ redox energy, which will be discussed below.

B. Atomic and electronic structure of $\alpha\text{-Pu}_2\text{O}_3$

$\alpha\text{-Pu}_2\text{O}_3$ in body-centered cubic structure is the end product during the reduction action process. The crystal

structure of $\alpha\text{-Pu}_2\text{O}_3$ is well confirmed by X-ray powder diffraction measurement [4, 5]. As mentioned above, after building the PuO_2 $2 \times 2 \times 2$ supercell and removing 25% oxygen atoms in special sites, $\alpha\text{-Pu}_2\text{O}_3$ can be obtained. Therefore, there are 32 plutonium atoms and 48 oxygen atoms in the unit cell for $\alpha\text{-Pu}_2\text{O}_3$ (see Fig. 1). The calculated structural and mechanical parameters within GGA+ U scheme with different Hubbard U parameters for $\alpha\text{-Pu}_2\text{O}_3$ are also collected in table I. We also performed the calculations in FM and AFM phases for $\alpha\text{-Pu}_2\text{O}_3$. For the AFM calculations, we adopted two different spin arrangements of plutonium ions. One spin arrangement is to confine μ along the z axis in a simple intra- or interlayer $+-+$ alternation of spins, as what we dealt with PuO_2 in the last section. Another model is to use the same spin arrangement as in $\alpha\text{-Mn}_2\text{O}_3$. Based on the neutron diffraction measurement, Regulski *et al.* [24] proposed a appropriate collinear AFM ordering, in which four basic magnetic cubic sublattices are constructed and the summation of magnetic moments of eight ions are assumed to be zero in each cube. We also adopt this AFM configuration as one additional candidate to calculate the total energy of $\alpha\text{-Pu}_2\text{O}_3$ as a function of U . The calculated lattice constant in the latter AFM ordering are 10.92, 11.17, and 11.20 Å for $U=0, 3.0, \text{ and } 4.0$ eV, and the corresponding bulk modulus are 123, 122, and 128 GPa, respectively. Note that the corresponding experimental lattice constant is in a range of 11.03 to 11.07 Å [4, 5]. We find that similar to PuO_2 , at Hubbard $U=0$ eV, the result obtained by bare GGA predicts $\alpha\text{-Pu}_2\text{O}_3$ to be a FM metal. Considering that traditional DFT approach within the bare GGA scheme underestimates the strong on-site Coulomb repulsion of plutonium $5f$ electrons and can not accurately describe the localization of $5f$ electrons, therefore, we conclude this result obtained by bare GGA is not correct although no magnetic susceptibility or neutron powder diffraction data are available. Further calculations show that at Hubbard $U=3.0$ eV and 4.0 eV, the ground state of $\alpha\text{-Pu}_2\text{O}_3$ is an AFM insulator (see below). Notice that our direct calculations show that the $\alpha\text{-Pu}_2\text{O}_3$ in AFM phase is preferred to the latter spin arrangement as mentioned above. The corresponding energy differences $\Delta E = E_{\text{AFM1}} - E_{\text{AFM2}}$ are 43 and 26 meV at $U=3.0$ and 4.0 eV per unit cell, respectively. As for the stability of AFM phase, the energy differences $\Delta E = E_{\text{AFM2}} - E_{\text{FM}}$ are -3.63 and -5.80 eV at $U=3.0$ and 4.0 eV per unit cell, respectively.

C. Changes in the electronic properties during reduction process

In PuO_2 and $\alpha\text{-Pu}_2\text{O}_3$, the ideal oxidation states of Pu ions are +4 and +3, respectively. This valence difference apparently shows that the population of $5f$ changes and in depth demonstrates that the behavior of Pu $5f$ is very complex. Directly, $\alpha\text{-Pu}_2\text{O}_3$ can be constructed

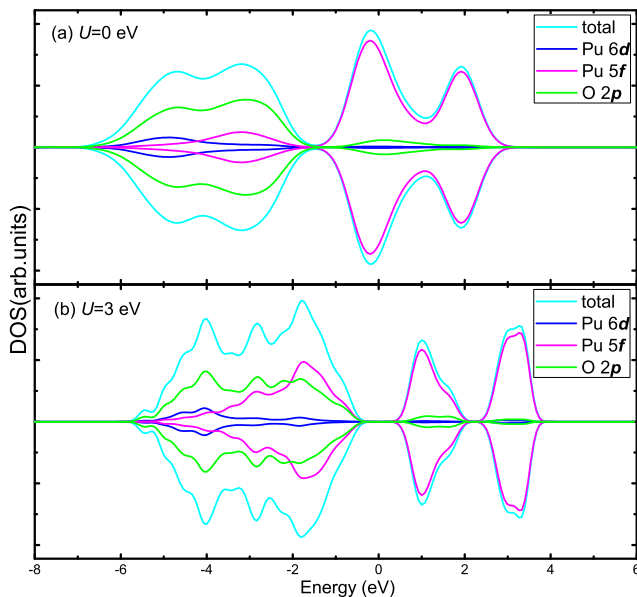


FIG. 3: The total DOS for AFM PuO_2 and projected orbital-resolved partial DOS for Pu $6d$, Pu $5f$, and O $2p$ at Hubbard (a) $U=0$ eV and (b) $U=3$ eV, respectively. The Fermi level is set to zero.

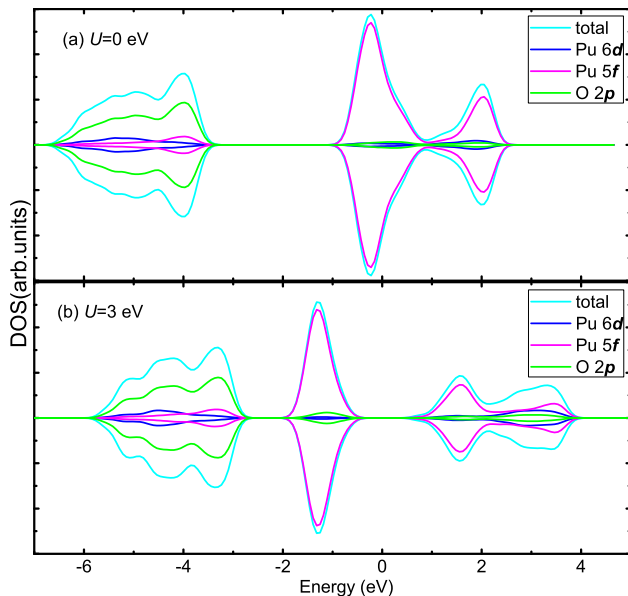


FIG. 4: The total DOS for AFM $\alpha\text{-Pu}_2\text{O}_3$ and projected orbital-resolved partial DOS for Pu $6d$, Pu $5f$, and O $2p$ at Hubbard (a) $U=0$ eV and (b) $U=3$ eV, respectively. The Fermi level is set to zero.

from PuO_2 by removing 25% oxygen atoms. After removing one oxygen atom, two additional electrons are left behind. These two electrons will occupy the lowest unoccupied states derived from Pu $5f$ orbitals. This leads to the fact that the population of f^5 forms in $\alpha\text{-Pu}_2\text{O}_3$, while f^4 in PuO_2 . This clearly illustrates that Pu $5f$ orbitals are more localized in $\alpha\text{-Pu}_2\text{O}_3$ compared

with PuO_2 . In the following, we systematically investigated how the electronic structures characterized by $5f$ electrons change from PuO_2 to $\alpha\text{-Pu}_2\text{O}_3$. In order to make comparison, the electronic structure properties of PuO_2 $2\times 2\times 2$ supercell containing 96 atoms are also calculated. We will show in detail how the volume of unit cell, density of states (DOS), charge distribution, valence state, and magnetic order change. All the following results are obtained by GGA+ U scheme with $U=3.0$ eV except extra hints.

(I) The calculated lattice constants for PuO_2 and $\alpha\text{-Pu}_2\text{O}_3$ in their AFM phase are 5.458 and 11.17 Å, leading to 7% volume expansion. This suggests that the $5f$ electrons are more localized in $\alpha\text{-Pu}_2\text{O}_3$. Due to the increasing localization, the interaction between Pu ions and the cohesion of the crystal decrease, therefore the lattice constant increases. The similar phenomenon has also been observed in the reduction process from Ce_2O_3 to CeO_2 with a 10% volume change [6] also because of the increasing localization of the f orbitals.

(II) The total DOS for PuO_2 (96 atoms) and $\alpha\text{-Pu}_2\text{O}_3$ (80 atoms) within GGA+ U scheme at different Hubbard U are shown in Figs. 3 and 4, respectively. In order to make a clear comparison, the orbital-resolved partial DOS for Pu $6d$, Pu $5f$, and O $2p$ orbitals are also plotted. As showed in Fig. 3(a), at $U=0$ eV, it is clearly that the bare GGA scheme predicts PuO_2 to be a metal, which is contrary to the experimentally established insulating ground state [18]. However, in Fig. 3(b), at Hubbard $U=3.0$ eV, one can see that the present result correctly predict PuO_2 to be an AFM insulator. As for $\alpha\text{-Pu}_2\text{O}_3$, at Hubbard $U=0$ eV showed in Fig. 4(a), the bare GGA approach predicts the FM metal ground state as we expected, which is supposed to be not reasonable by considering the necessity of the Hubbard U correction. At Hubbard $U=3.0$ eV, the calculated DOS showed in Fig. 4(b) again suggests $\alpha\text{-Pu}_2\text{O}_3$ to be in the insulating AFM ground state. Concerning the satisfactory description of the electronic structures for PuO_2 and the fact that the $5f$ electrons in $\alpha\text{-Pu}_2\text{O}_3$ are more localized than in PuO_2 , we predict $\alpha\text{-Pu}_2\text{O}_3$ to be an insulator in the AFM state, although no experimental data can be obtained.

As for the projected orbital-resolved partial DOS showed in Fig. 3(b) for PuO_2 , the occupied DOS is featured by two well-resolved peaks. One near -1.8 eV is dominated by Pu $5f$ character, while another one near -4.0 eV is mostly O $2p$, which have observed in the recent photoemission measurement [9]. One can see that Pu $6d$, Pu $5f$, and O $2p$ states (especially between Pu $5f$ and O $2p$) shows a significant hybridization covering from -5.7 to -0.4 eV. This hybridization is also responsible for the strong covalency of PuO_2 . However, for $\alpha\text{-Pu}_2\text{O}_3$, the Pu($5f$)-O($2p$) hybridization is much smaller due to the fact that Pu $5f$ and O $2p$ occupied states are well separated as showed in Fig. 4(b). Furthermore, the covalency in $\alpha\text{-Pu}_2\text{O}_3$ is weaker than PuO_2 , which can also be demonstrated by the charge density distribution discussed below. We also note that in $\alpha\text{-Pu}_2\text{O}_3$, the oc-

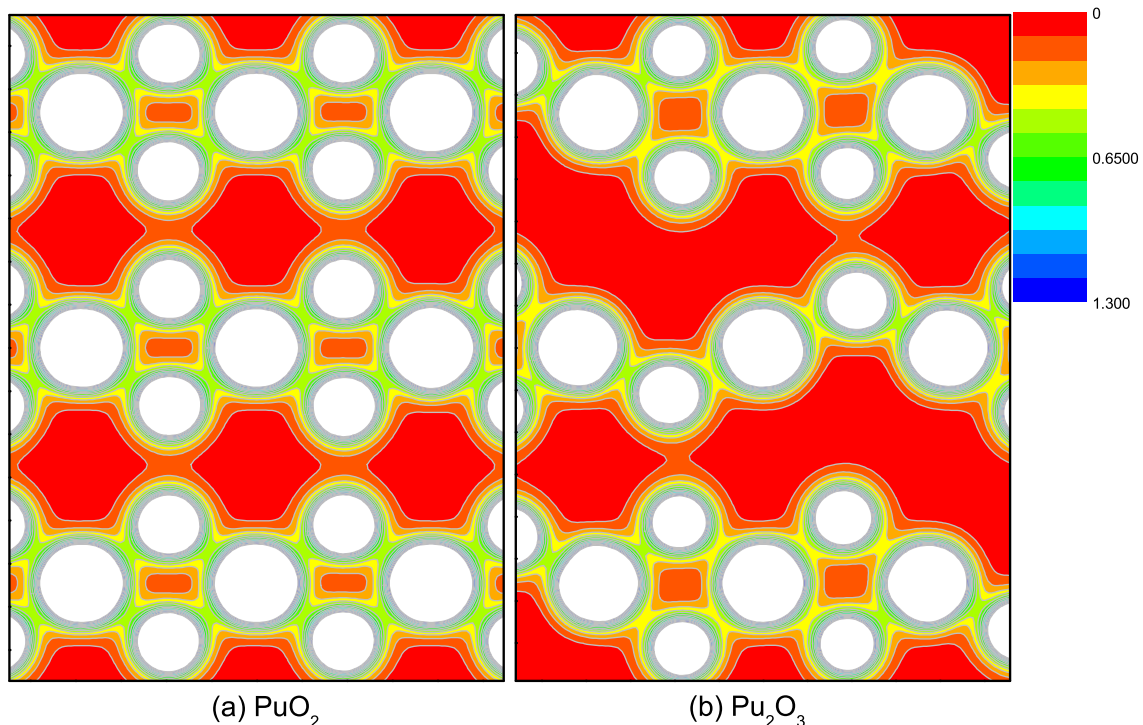


FIG. 5: Charge density in the (110) plane for (a) PuO_2 and (b) $\alpha\text{-Pu}_2\text{O}_3$, respectively. The contour lines are plotted from 0.000 to 1.300 by the interval of $0.1083 \text{ e}/\text{\AA}^3$.

cupied $5f$ peak around -1.3 eV is very narrow, indicating that the $5f$ orbitals are very localized, which is consistent with the conclusion in above part (I).

(III) In order to obtain further understanding of the electronic structure and bonding properties, the contours of the charge densities in the (110) plane are also plotted for AFM PuO_2 and AFM $\alpha\text{-Pu}_2\text{O}_3$ in Figs. 5(a) and 5(b), respectively. Note that the contour lines are plotted from 0.000 to 1.300 by the interval of $0.1083 \text{ e}/\text{\AA}^3$. For PuO_2 in Fig. 5(a), it is evident that there are some closed contours existing between Pu and O atoms. This suggests that the covalent bonding character exists in PuO_2 as discussed in above part (II). Compared with the charge density distribution for $\alpha\text{-Pu}_2\text{O}_3$ showed in Fig. 5(b), one can see that the charge density at most bridges connecting Pu and O atoms are larger in PuO_2 than in $\alpha\text{-Pu}_2\text{O}_3$, this demonstrates that the covalency is much stronger in the former. Note that the distribution of charge density around Pu atoms is nearly spherical, while the distribution around O atoms is a little deformed towards their bonds. Therefore, it is easy to decide their ionic radii according the minimum value of charge density along the nearest Pu-O bond. Then we can obtain the valence states for Pu ions discussed below.

(IV) For PuO_2 and $\alpha\text{-Pu}_2\text{O}_3$, there are 12.463 and 12.835 electrons around the plutonium ions with ionic radii of 1.287 and 1.319 \AA , therefore, the plutonium ions are presented as $\text{Pu}^{3.54+}$ and $\text{Pu}^{3.16+}$, which are close to the corresponding ideal valence states $+4$ and $+3$ for plutonium ions, respectively.

(V) As for the magnetic order, we notice for PuO_2 ($2 \times 2 \times 2$ supercell) the second spin arrangement model is also more energetically favored with the energy difference $\Delta E = E_{\text{AFM1}} - E_{\text{AFM2}}$ of 0.733 and 0.372 eV (per $2 \times 2 \times 2$ supercell) at Hubbard $U = 3.0$ and 4.0 eV, respectively. As for $\alpha\text{-Pu}_2\text{O}_3$, the corresponding energy differences $\Delta E = E_{\text{AFM1}} - E_{\text{AFM2}}$ are 43 and 26 meV at $U = 3.0$ and 4.0 eV per unit cell, respectively. Our direct calculations show that the magnetic moments are about 4.2 and 5.0 μ_B per Pu ion in PuO_2 and $\alpha\text{-Pu}_2\text{O}_3$, which are mainly contributed by $5f$ electrons of 4.1 and 5.0 μ_B and very close to the corresponding populations of f^4 and f^5 for plutonium ions, respectively. Notice that all the results of AFM phase listed in Figs. 3, 4, and 5 are obtained by the second spin arrangement model because it is energetically favored.

D. Reduction reaction energy

To further know the thermodynamic properties of the reduction process from PuO_2 to $\alpha\text{-Pu}_2\text{O}_3$ via the reaction



we have calculated the reaction energy $\Delta E = E_{\text{Pu}_2\text{O}_3} - E_{\text{PuO}_2} + 8E_{\text{O}_2}$ at Hubbard $U = 3.0 \text{ eV}$. Note that $E_{\text{Pu}_2\text{O}_3}$, E_{PuO_2} , and E_{O_2} are the total energies for Pu_2O_3 (unit cell), PuO_2 ($2 \times 2 \times 2$ supercell), and (spin-polarized) oxygen molecule, respectively. Considering the overestimation of the binding energy for O_2 introduced by DFT,

we use the experimental cohesive energy value of 5.21 eV for O₂ [25]. Finally, the reaction energy is 55.04 eV (per α -Pu₂O₃ unit cell). This indicates that the reaction is endothermic, which is consistent with the fact that α -Pu₂O₃ can be experimentally obtained by partial reduction of PuO₂ at high temperature [5].

IV. SUMMARY

In summary, we have studied the structural, electronic, and thermodynamics properties of PuO₂ and α -Pu₂O₃ in their antiferromagnetic insulator states. We find that after partial oxygen atoms removed from PuO₂, the left electrons are localized into the Pu 5*f* orbitals. As a consequence, several physical properties have changed correspondingly listed in following. (1) In PuO₂, the ideal valence state for Pu is +4, while in α -Pu₂O₃, the valence state is +3. Our charge density integration around Pu ion sphere also confirms this conclusion. (2) The magnetic

moments per Pu ion increase from 4 μ_B for PuO₂ to 5 μ_B for α -Pu₂O₃, which correspond to the populations of f^4 and f^5 , respectively. (3) Due to the more localization of 5*f* electrons, which do not contribute to the chemical bonding, thus the cohesion of α -Pu₂O₃ decreases. As a result, the volume expands about 7% according to our calculation. (4) Because of more localization of 5*f* orbitals, the occupied Pu 5*f* and O 2*p* orbitals are well separated, the hybridization between them decreases. Finally the covalency of the Pu-O bond in α -Pu₂O₃ is weakened. The calculated DOS and charge density distribution also demonstrate this.

Acknowledgments

This work was supported by the Foundations for Development of Science and Technology of China Academy of Engineering Physics.

-
- [1] S. Y. Savrasov and G. Kotliar, Phys. Rev. Lett. **84**, 3670(2000).
 - [2] K. T. Moore and G. van der Laan, Rev. Mod. Phys. **81**, 235 (2009).
 - [3] J. M. Haschke, T. H. Allen, and L. A. Morales, Los Alamos Sci. **26**, 253 (2000).
 - [4] W. H. Zachariasen, Metallurgical Laboratory Report, CK-1367, 1944.
 - [5] IAEA technical reports series, No. 79 (1967).
 - [6] N.V. Skorodumova, S. I. Simak, B. I. Lundqvist, I. A. Abrikosov, and B. Johansson, Phys. Rev. Lett. **89**, 166601 (2002).
 - [7] S. L. Dudarev, G. A. Botton, S. Y. Savrasov, C. J. Humphreys, and A. P. Sutton, Phys. Rev. B **57**, 1505 (1998).
 - [8] B. Sun, P. Zhang, and X.-G. Zhao, J. Chem. Phys. **128**, 084705 (2008).
 - [9] M. Butterfield, T. Durakiewicz, E. Guziewicz, J. Joyce, A. Arko, K. Graham, D. Moore, and L. Morales, Surf. Sci. **571**, 74 (2004).
 - [10] Gérald. Jomard, B. Amadon, Francois Bottin, and M. Torrent, Phys. Rev. B **78**, 075125 (2008).
 - [11] D. A. Andersson, J. Lezama, B. P. Uberuaga, C. Deo, and S. D. Conradson, Phys. Rev. B **79**, 024110 (2009).
 - [12] L. Petit, A. Svane, Z. Szotek, W. M. Temmerman, and G. M. Stocks, arXiv:0908.1806v1 [cond-mat.str-el]
 - [13] M. Idiri, T. Le Bihan, S. Heathman, and J. Rebizant, Phys. Rev. B **70**, 014113 (2004).
 - [14] J.-P. Dancausse, E. Gering, S. Heathman, and U. Benedict, High Pressure Research **2**, 381 (1990).
 - [15] G. Kresse and J. Hafner, Phys. Rev. B **48**, 13115 (1993).
 - [16] Y. Wang and J.P. Perdew, Phys. Rev. B **44**, 13298 (1991).
 - [17] G. Kresse, D. Joubert, Phys. Rev. B **59**, 1758 (1999).
 - [18] C. E. McNeilly, J. Nucl. Mater. **11**, 53 (1964).
 - [19] P. Santini, R. Lemanski, and P. Erdos, Adv. Phys. **48**, 537 (1999); M. Colarieti-Tosti, O. Eriksson, L. Nordstrom, J. Wills, and M. S. S. Brooks, Phys. Rev. B **65**, 195102 (2002).
 - [20] F. Birch, Phys. Rev. **71**, 809 (1947).
 - [21] R. G. Haire and J. M. Haschke, MRS Bull. **26**, 689 (2001).
 - [22] I. D. Prodan, G. E. Scuseria, and R. L. Martin, Phys. Rev. B **73**, 045104 (2006).
 - [23] J. Cable, M. Wilkinson, E. Woolan, W. Koehler, Phys. Prog. Rep. **43** ORNL-2302 (1957).
 - [24] M. Regulski, R. Przenioslo, I. Sosnowska, D. Hohlwein, R. Schneider, J. Alloy. Compoun. **362**, 236 (2004).
 - [25] K. Huber, American Institute of Physics Handbook, edited by D. E. Gray(McGraw-Hill, New York, 1972).